Al-Furat Journal of Innovations in Electronics and Computer Engineering (FJIECE)
ISSN -2708-3985

Artificial Intelligence for Power Consumption Optimization in Reconfigurable Intelligent Surface-Assisted Communication Systems

Jehan Kadhim Shareef Al-Safi [1]

[1] University of Thi-Qar, Faculty of Media, Department of Digital Media, 64001, Iraq.
E-mail: jihan.k.shareef@utq.edu.iq , jihansh2020@gmail.com ,
Corresponding author E-mail: jihan.k.shareef@utq.edu.iq , jihansh2020@gmail.com

Article's Information

Received: 2.03.2026
Accepted: 28.03.2026
Published: 31.03.2026

Keywords:
Alternating Optimization
Educational Competition Optimizer
Energy Efficiency
Metaheuristic Optimization
Optimization Algorithm
Reconfigurable Intelligent Surface

Abstract

Intelligent and flexible resource management systems will be required as Sixth-Generation (6G) wireless networks advance in order to minimize energy consumption and safeguard against security risks. To reduce power consumption in active symbiotic secure communication networks, this study uses Reconfigurable Intelligent Surfaces (RIS) to improve the performance of Successive Interference Cancellation (SIC). Because it offers reliable, scalable, and nearly perfect solutions to this complex, non-convex, multi-variable optimization problem, artificial intelligence is essential. We use the Educational Competition Optimizer (ECO), a unique metaheuristic algorithm based on human cognition, to determine the optimal values for the beamforming vector and the active RIS reflection coefficient matrix. The algorithm finds a good balance between exploration and exploitation by simulating how competition changes over time in elementary, middle, and high school. The simulation results show that the proposed AI-driven approach uses 89.0% less power than traditional passive RIS, 52.5% less power than active RIS with random phases, 12.8% less power than Alternating Optimization with Successive Convex Approximation (AO SCA), 10.1% less power than hybrid Particle Swarm Optimization Grey Wolf Optimizer (PSO GWO), and 4.7% less power than hybrid Deep Neural Network Genetic Algorithm Deep Reinforcement Learning (DNN GA DRL). It also meets all security and reliability requirements with 100% feasibility. These results show that AI has the power to change how we communicate in the future by developing systems that are safe, energy-efficient, and long-lasting.

https://doi.org/10.46649/fjiece.v5.1.11a.31.3.2026
*Corresponding author: jihan.k.shareef@utq.edu.iq , jihansh2020@gmail.com

1. INTRODUCTION

Connecting to Sixth-Generation (6G) wireless networks will be very different. There will be more devices than ever before, and they will use a lot less power. One new technology that could help achieve these goals is Symbiotic Radio (SR). It uses both cognitive radio and backscatter communication [1]–[3]. In SR networks, the main and secondary systems work together. The secondary system leverages the primary system's energy and spectrum resources. It adds multipath components to improve the primary transmission. This mutually beneficial relationship is a strong answer to the problems of high infrastructure costs, high energy use, and limited spectrum that are common in the Internet of Things (IoT) era [4]–[6].

In theory, SR systems could work, but several technical issues make them hard to use. People can always listen in on these systems because wireless channels are broadcast. Sharing resources is even harder when there are strict rules about how reliable secondary communications need to be. Reconfigurable intelligent surfaces (RISs) are a promising approach to addressing these problems because they enable the modification of electromagnetic wave propagation [7]–[9]. There are many inexpensive passive or active reflectors in RISs. They can change the routes signals take to improve the transmissions they want while also preventing eavesdropping and interference. Active RISs with built-in amplifiers offer unique benefits because they do not suffer from the strong double-fading effect that makes passive setups less useful. This helps them get much better coverage and stronger signals [10], [11].

It is not easy to figure out how to get the most out of active RIS-assisted symbiotic secure communication systems. The joint design of the primary transmitter beamforming vector and the RIS reflection coefficient matrix is characterized by highly nonconvex constraints, interdependent variables, and uncertain parameters arising from suboptimal SIC [12]–[14]. One of the traditional optimization methods that works well but is often hard to use, sensitive to initialization, and not very scalable is alternating optimization with successive convex approximation [15]–[17]. These problems show that we need smart, adaptable methods that can quickly and accurately navigate complex solution spaces.

Metaheuristic optimization demonstrates that AI offers a novel approach to addressing complex resource-allocation problems [18], [19]. Metaheuristic algorithms that use AI do not employ derivatives, making them more effective at navigating non-convex, discontinuous, or high-dimensional spaces than conventional gradient-based approaches [20], [21]. There are many different types of metaheuristic algorithms. The best ones are on the ideas of choice-based learning and competition [22], [23]. These algorithms automatically find a balance between exploration (the ability to search the solution space broadly) and exploitation (the ability to improve promising solutions) by mimicking how people naturally behave [24].

Recent studies have examined the potential contributions of AI and RIS to various components of wireless networks. Ahmed et al. [25] conducted a comprehensive study on Simultaneous Transmitting and Reflecting RIS (STAR-RIS) in 2023. They examined its current utilization and potential future challenges. Zhang et al. [26] examined methods to enhance the security of coupled phase-shift STAR-RIS networks. Mohsin et al. [27] also created a Deep Reinforcement Learning (DRL) framework for RIS-integrated networks on the ground and in space that year. The basis for this framework is Hybrid Proximal Policy Optimization (H-PPO), which had a significant impact on both the total rate and the energy consumption. In 2024, Hazarika et al. [28] and Mirza et al. [29] examined DRL-driven task offloading in RIS-assisted vehicular edge computing networks. Ayub et al. [30] enhanced RIS-assisted 6G non-terrestrial networks to facilitate communication among uncrewed aerial vehicles (UAVs) during their mobility. Zaoutis et al. [31] examined AI-controlled RIS in 6G wireless communications in 2025. They switched from supervised to federated learning models. Padial-Allué et al. [32] recently demonstrated a method to expedite RIS configuration using Field-Programmable Gate Array (FPGA) platforms by integrating hardware and deep learning. They could set up more than 18,000 times per second.

The hybrid Particle Swarm Optimization with Grey Wolf Optimizer (PSO-GWO) for RIS phase-shift design [33] and the hybrid DNN-GA-DRL framework for optimizing resource allocation and RIS deployment [34] are two examples of complementary hybrid metaheuristic approaches that demonstrate the effectiveness of combining evolutionary search with artificial intelligence (AI).

Even with these improvements, there has not been much research on how to make active RIS-assisted symbiotic secure communication systems work better in the real world. For example, when Successive Interference Cancellation (SIC) does not work as it should. Most of the time, existing work uses either traditional convex optimization or methods that switch between optimization and non-optimization. It is hard to understand these methods because they depend on how they are prepared, and they do not work

well in places that change quickly. AI has not fully resolved these intricate, interdependent resource-allocation challenges, particularly those grounded in human metaheuristics.

This study proposes an AI-driven framework for resource allocation based on the ECO [23] to address the issue. The ECO algorithm examines how competition evolves across elementary, middle, and high school levels to find a good balance between exploration and exploitation. Even when SIC is not perfect, the suggested method reduces the system's overall power consumption while keeping the primary signal safe and the secondary signal reliable by jointly optimizing the primary transmitter beamforming vector and the active RIS reflection coefficient matrix. The three contributions are: (1) making a strong power minimization problem with real-world limits; (2) making a penalty-based ECO algorithm that can handle different types of encoding and limits; and (3) running a lot of tests that show the algorithm works better than standard and state-of-the-art benchmarks, like passive RIS, active RIS with random phases, the Alternating Optimization (AO) Algorithm with Successive Convex Approximation (SCA) (AO-SCA), hybrid PSO-GWO, and hybrid DNN-GA-DRL.

The rest of this paper is the same. Part 2 tells how to share resources and what the system model looks like. In Section 3, we will talk about the ECO-based AI solution. We talk about where it came from, how math was used to make it, how variables were encoded, how it was added to the problem, and algorithmic pseudocode. We discuss how the simulation was set up, how it converged, which parameters affected it, and how it compared to benchmark methods in Section 4. Section 5 of the paper discusses the conclusions and what should happen next in the research.

2. SYSTEM MODEL AND PROBLEM FORMULATION

2.1. SYSTEM DESCRIPTION

In this study, we present a secure communication system comprising an active Reconfigurable Intelligent Surface (RIS) with reflecting elements (N), a primary transmitter (PTx) with antennas (K), a single-antenna receiver (IR), and a single-antenna eavesdropper (Eve). The secure primary system comprises the PTx and IR, while the sensing secondary system comprises the active RIS and IR. The PTx sends private primary signals, and the active RIS simultaneously boosts them to improve primary communication. It also works as a secondary transmitter, sending secondary information using backscatter technology [1]–[3], [11] and using the primary signal as a carrier.

The reflection coefficient matrix of the active RIS is denoted by $Q = \mathrm{diag}\left(\beta_1 e^{j\theta_1}, \beta_2 e^{j\theta_2}, \dots, \beta_N e^{j\theta_N}\right)$, where ($\theta_n \in [0,2\pi]$ and $\beta_n \geq 1$) represent the phase shift and amplification coefficient of the n-th reflecting element, respectively. The ability to amplify signals distinguishes active configurations from passive ones; this helps the system compensate for path loss and also makes the thermal noise from the built-in amplifiers more pronounced [10], [11].

We believe that all channels exhibit quasi-static block fading, indicating that the channel coefficients remain constant within each fading block while varying independently between blocks. The channel from PTx to RIS is $\boldsymbol{H}_{ps} \in \mathbb{C}^{N\times K}$, and the channels from RIS to IR and from RIS to Eve are $\boldsymbol{h}_{si} \in \mathbb{C}^{N\times 1}$ and $\boldsymbol{h}_{se} \in \mathbb{C}^{N\times 1}$, respectively. The direct channels from PTx to IR and from PTx to Eve are denoted by $h_{pi} \in \mathbb{C}^{K\times 1}$ and $h_{pe} \in \mathbb{C}^{K\times 1}$, respectively. Figure 1 illustrates the system model.

Al-Furat Journal of Innovations in Electronics and Computer Engineering (FJIECE)
ISSN -2708-3985

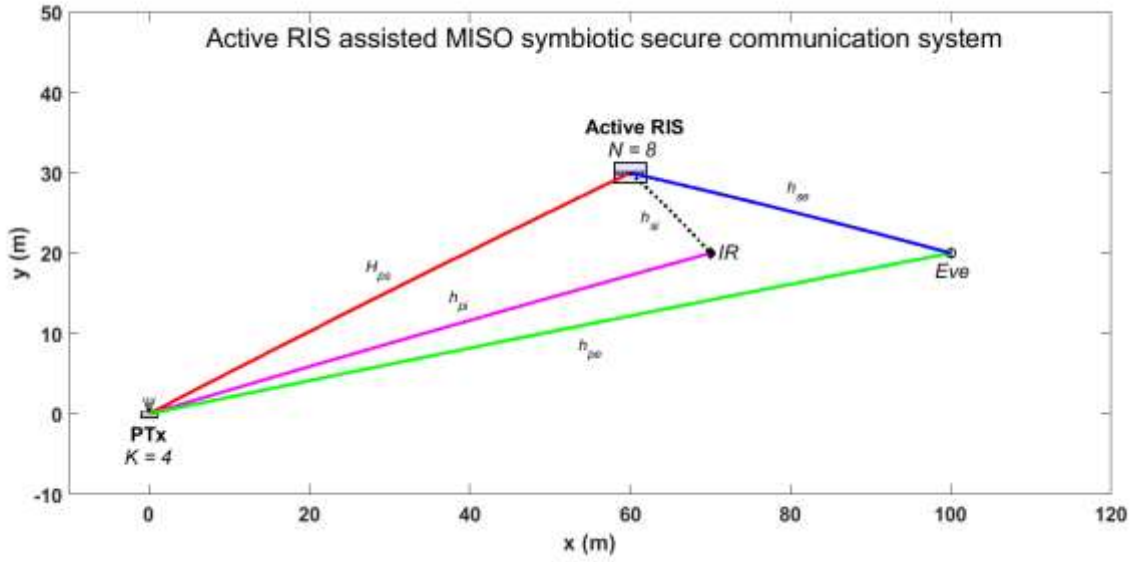

Figure 1. Active RIS-assisted Multiple-Input Single-Output (MISO) symbiotic secure communication system.

This Figure illustrates the system model under investigation. The primary transmitter (PTx) is equipped with antennas (K) and communicates with an intended receiver (IR) and an eavesdropper (Eve). An active RIS comprising reflecting elements (N) is deployed to assist both primary and secondary transmissions. The PTx transmits confidential primary signals, while the active RIS simultaneously amplifies them to enhance primary communication and serves as a secondary transmitter via backscatter. The channels are labeled as follows: $\boldsymbol{H}_{ps}$(PTx to RIS), $\boldsymbol{h}_{si}$(RIS to IR), $\boldsymbol{h}_{se}$(RIS to Eve), $\boldsymbol{h}_{pi}$(PTx to IR), and $\boldsymbol{h}_{pe}$ (PTx to Eve). The Figure also shows the direct and reflected links, indicating that the active RIS can perform two functions: amplify signals and transmit secondary information.

2.2. SIGNAL AND RATE ANALYSIS

For secondary transmission, the RIS uses binary phase shift modulation, and the secondary signal is $c \in \{-1,1\}$. Let T_s and T_c represent the symbol periods for primary and secondary transmissions, respectively, satisfying $T_c = LT_s$ with $L \gg 1$. Under strict synchronization, the PTx sends L primary signals within one secondary signal period. The signals received at IR and Eve can be expressed as [8], [12]:

$$y_i(l) = \left(\boldsymbol{h}_{pi}^H + \boldsymbol{h}_{si}^H \boldsymbol{Q} \boldsymbol{H}_{ps}\right)\boldsymbol{w}s(l) + \boldsymbol{h}_{si}^H \boldsymbol{Q}\boldsymbol{n}_A(l) + n_i(l) \quad (1)$$

$$y_e(l) = \left(\boldsymbol{h}_{pe}^H + \boldsymbol{h}_{se}^H \boldsymbol{Q} \boldsymbol{H}_{ps}\right)\boldsymbol{w}s(l) + \boldsymbol{h}_{se}^H \boldsymbol{Q}\boldsymbol{n}_A(l) + n_e(l) \quad (2)$$

where $w \in \mathbb{C}^{K\times 1}$ is the beamforming vector at PTx, $s(l)$ is the primary signal with $\mathbb{E}\{|s(l)|^2\} = 1$, $\boldsymbol{n}_A(l) \sim \mathcal{CN}(\boldsymbol{0}, \sigma_A^2 \boldsymbol{I})$ does the active RIS generate the thermal noise, and $n_i(l) \sim \mathcal{CN}(0, \sigma_i^2)$, $n_e(l) \sim \mathcal{CN}(0, \sigma_e^2)$ are the additive white Gaussian noise at IR and Eve, respectively.

IR uses joint decoding for both primary and secondary signals. To decode the primary signal, the reflected link is a multipath component seen, which gives the Signal-to-Noise Ratio (SNR) [8], [11]:

Al-Furat Journal of Innovations in Electronics and Computer Engineering (FJIECE)
ISSN -2708-3985

$$\gamma_s = \frac{\left|\left(h_{\mathrm{pi}}^H + h_{\mathrm{si}}^H Q H_{\mathrm{ps}}\right)w\right|^2 + \left|\left(h_{\mathrm{pi}}^H - h_{\mathrm{si}}^H Q H_{\mathrm{ps}}\right)w\right|^2}{2\left(\sigma_i^2 + \left\|h_{\mathrm{si}}^H Q\right\|^2 \sigma_A^2\right)} \quad (3)$$

The corresponding achievable rate at IR is $R_{i,s} = \log_2(1+\gamma_s)$. The achievable rate for Eve, which targets the main signal, is [12], [14]:

$$R_{e,s} = \log_2\left(1 + \frac{\left|(h_{\mathrm{pe}}^H + h_{\mathrm{se}}^H Q H_{\mathrm{ps}})w\right|^2 + \left|(h_{\mathrm{pe}}^H - h_{\mathrm{se}}^H Q H_{\mathrm{ps}})w\right|^2}{2\left(\sigma_e^2 + \left\|h_{\mathrm{se}}^H Q\right\|^2 \sigma_A^2\right)}\right) \quad (4)$$

The achievable secrecy rate of the primary signal is then $R_s = \max\left(R_{i,s} - R_{e,s}, 0\right)$ [12], [14].

After successfully decoding the main signal, IR uses Successive Interference Cancellation (SIC) to decode the secondary signal. Because of hardware limitations, a perfect SIC is not possible, leaving interference from the direct link [13], [16]. The Signal-To-Interference-Plus-Noise Ratio (SINR) for secondary signal decoding is approximated as:

$$\gamma_c \approx \frac{L\left|(h_{\mathrm{si}}^H Q \boldsymbol{H}_{\mathrm{ps}})w\right|^2}{\mu\left|h_{\mathrm{pi}}^H w\right|^2 + \sigma_i^2 + \left\|h_{\mathrm{si}}^H Q\right\|^2 \sigma_A^2} \quad (5)$$

where $0 \le \mu < 1$ is the SIC factor representing residual interference strength [13].

2.3. OPTIMIZATION PROBLEM FORMULATION

The goal is to use as little power as possible while ensuring the main signal remains safe, and the secondary signal remains reliable. The total power is the sum of the PTx power and the power used by the active RIS to boost signals and reduce thermal noise.

The optimization problem is formulated as [10], [14]:

$$\left.\begin{aligned} \min_{w,Q} \quad & \|w\|^2 + \left\|Q\boldsymbol{H}_{\mathrm{ps}}\boldsymbol{w}\right\|^2 + \|\boldsymbol{Q}\|_F^2 \sigma_A^2 \\ \text{s.t.} \quad & C1: \boldsymbol{R}_s \ge R_s^{\min} \\ & C2: \gamma_c \ge \gamma_c^{\min} \\ & C3: \left\|\boldsymbol{Q}\boldsymbol{H}_{\mathrm{ps}}\boldsymbol{w}\right\|^2 + \|\boldsymbol{Q}\|_F^2 \sigma_A^2 \le P_I \\ & C4: \beta_n \ge 1, \theta_n \in [0, 2\pi], \forall n \in \mathcal{N} \end{aligned}\right\} \quad (6)$$

$R_s^{\min}$ is the lowest secrecy rate needed for the main signal (in bits per second), $\gamma_c^{\min}$ is the minimum SINR required for the secondary signal (on a linear scale), and P_I is the maximum power budget for the active RIS. Constraint $C1$ makes sure that the main transmission is safe, $C2$ makes sure that the secondary service is good, $C3$ limits how much power the RIS can use, and $C4$ makes sure that the reflecting elements can change the phase and amplify. In this case, the set of reflecting elements is $\mathcal{N} = \{1, 2, \ldots, N\}$.

There are a few factors that worsen the problem, such as an error in sequential interference cancellation that makes people less certain, the dependence of the optimization variables, and the non-convex secrecy rate constraint [14]-[16]. The only way to come up with useful answers in this tough area is to move slowly.

Al-Furat Journal of Innovations in Electronics and Computer Engineering (FJIECE)
ISSN -2708-3985

3. ARTIFICIAL INTELLIGENCE-DRIVEN RESOURCE ALLOCATION USING EDUCATIONAL COMPETITION OPTIMIZER

3.1. ALGORITHMIC INSPIRATION AND PRINCIPLES

The Educational Competition Optimizer (ECO) is a metaheuristic algorithm that draws on the principles of academic competition. The level of competition among kids increases significantly as they move from elementary school to middle school and then to high school; this affects both what kids learn and how they learn it. The three-stage optimization process starts with exploration and ends with targeted exploitation after a phase of balanced exploration and exploitation [22], [23].

The ECO search engine was made possible by people working together. The majority of people are students, and the most knowledgeable people are teachers; this is how the method sorts the population. The algorithm's gradual decrease in the number of schools indicates that more educated consumers are more selective [23]. To simulate the changing competitive landscape, three different update mechanisms are used in cycles to represent the stages of elementary, middle, and high school.

3.2. MATHEMATICAL FORMULATION OF SEARCH MECHANISMS

ECO uses logistic chaos mapping to establish the population, ensuring high diversity and preventing early convergence [23]. For a population size (M) and problem dimension (D), the initial positions are generated as [23]:

$$x_i = \alpha \cdot x_{i-1} \cdot (1 - x_{i-1}), 0 \le x_0 \le 1, i = 1,2,\cdots,M, \alpha = 4 \quad (7)$$

followed by mapping to the search space [23]:

$$X_i = lb + (ub - lb).x_i \quad (8)$$

where ***lb*** and ***ub*** are the lower and upper limits of the decision variables, respectively [23].

The algorithm runs for a set number of Iterations (T). At each iteration, the algorithm evaluates each candidate solution and sorts the population accordingly. A decreasing threshold determines which schools are chosen: in the primary stage, the top 20% are selected; in the middle and high school stages, the top 10% are selected [23].

Depending on the iteration index modulo 3, the three educational levels—elementary, middle, and high school—were adjusted to balance exploration and exploitation; this is done in accordance with the primary objective. To identify potential areas, the algorithm employs a three-tiered educational competition. In elementary school, there is a broad exploration phase; in middle school, a refinement phase to keep things interesting; and in high school, a strict exploitation phase to identify the best solutions. The modulo-3 cycle causes the program to return to each behavioral level repeatedly. To prevent any phase from becoming stuck too soon, this maintains the proper balance between exploration and exploitation. This cyclical pattern was supported by the original ECO study [23]. Because active symbiotic secure communication systems that employ a Reconfigurable Intelligent Surface (RIS) typically have a very non-convex, interconnected solution space, you must be able to investigate this field. The iteration index modulo 3 controls each of the three components of the search.

Stage 1: Primary school ($t \equiv 1(\mathrm{mod}3)$)

Schools change their positions by moving toward the average position of the population with a Levy flight perturbation [23]:

$$\boldsymbol{X}_i^{t+1} = \boldsymbol{X}_i^t + \delta \cdot \left(\boldsymbol{X}_{i,\,\mathrm{mean}}^t - \boldsymbol{X}_i^t\right) \cdot \mathrm{Levy}(D) \quad (9)$$

Al-Furat Journal of Innovations in Electronics and Computer Engineering (FJIECE)
ISSN -2708-3985

where $\delta = 0.1\ln(2 - t/T)$ is an adaptive step size, $X_{i,\text{mean}}^{v}$ is the element-wise mean of the school's current position vector, and Levy(D) generates Lévy-distributed random steps. The Lévy flight step makes heavy-tailed jumps that help with exploration; see the original ECO reference [23] for more information. Students update to the nearest school [23]:

$$\boldsymbol{X}_i^{t+1} = \text{close}(\boldsymbol{X}_i^t) + \text{randn} \cdot \left|\boldsymbol{X}_{i,\text{mean}}^t - \text{close}(\boldsymbol{X}_i^t)\right| \quad (10)$$

where close $(\boldsymbol{X}_i^t)$ denotes the position of the school closest to the student.

Stage 2: Middle school ($t \equiv 2(\text{mod}3)$)

Schools adopt a more sophisticated update incorporating both the population mean and the best-known position [23]:

$$\boldsymbol{X}_i^{t+1} = \boldsymbol{X}_i^t + (\boldsymbol{X}_{\text{best}}^t - \boldsymbol{X}_{\text{mean}}^t) \cdot \exp\left(\frac{t}{T} - 1\right) \cdot \text{Levy}(D) \quad (11)$$

Students are categorized based on their learning patience parameter $P = 4 \cdot \text{randn} \cdot (1 - t/T)$ and a binary classification determined by a random threshold. Gifted students (with motivation $E = \pi/P \cdot t/T$) receive differentiated updates [23]:

$$\boldsymbol{X}_i^{t+1} = \begin{cases} \boldsymbol{X}_i^t - \delta \cdot \text{close}(\boldsymbol{X}_i^t) - P \cdot (E \cdot \delta \cdot \text{close}(\boldsymbol{X}_i^t) - \boldsymbol{X}_i^t), & R_1 < 0.5 \\ \boldsymbol{X}_i^t - \delta \cdot \text{close}(\boldsymbol{X}_i^t) - P \cdot (\delta \cdot \text{close}(\boldsymbol{X}_i^t) - \boldsymbol{X}_i^t), & R_1 \geq 0.5 \end{cases} \quad (12)$$

Stage 3: High school $(t \equiv 0(\text{mod}3))$

Schools refine their positions with consideration of the best and worst positions in the population [23]:

$$\boldsymbol{X}_i^{t+1} = \boldsymbol{X}_i^t + (\boldsymbol{X}_{\text{best}}^t - \boldsymbol{X}_i^t) \cdot \text{randn} - (\boldsymbol{X}_{\text{best}}^t - \boldsymbol{X}_i^t) \cdot \text{randn} \quad (13)$$

All students converge toward the best school [23]:

$$\boldsymbol{X}_i^{t+1} = \begin{cases} \boldsymbol{X}_{\text{best}}^t - P \cdot (E \cdot \boldsymbol{X}_{\text{best}}^t - \boldsymbol{X}_i^t), & R_2 < 0.5 \\ \boldsymbol{X}_{\text{best}}^t - P \cdot (\boldsymbol{X}_{\text{best}}^t - \boldsymbol{X}_i^t), & R_2 \geq 0.5 \end{cases} \quad (14)$$

Throughout the optimization, a greedy selection mechanism ensures that only improvements are retained, preventing degradation of solution quality [23].

3.3. ENCODING OF OPTIMIZATION VARIABLES

To apply ECO, the optimization variables ($\boldsymbol{w}, \boldsymbol{Q}$) must be encoded into a real-valued decision vector (X) of dimension $D = 2K + 2N$. Specifically:

- The beamforming vector $\boldsymbol{w} \in \mathbb{C}^{\boldsymbol{K}}$ is represented by its real and imaginary parts: $\boldsymbol{w} = \Re(\boldsymbol{w}) + j\Im(\boldsymbol{w})$. These $2K$ real numbers occupy the first $2K$ positions of $\boldsymbol{X}$.
- The reflection coefficient matrix $\boldsymbol{Q} = \text{diag}\left(\beta_1 e^{j\theta 1}, \ldots, \beta_N e^{j\theta N}\right)$ is encoded by the amplitudes β_n and phases θ_n (in radians). These $2N$ real numbers occupy the remaining positions of $\boldsymbol{X}$.
- Bounds: For the beamforming vector components, the bounds are $\pm\sqrt{P_{\max}}$ (where $P_{\max}$ is a sufficiently large value e.g., 10), ensuring feasibility. For β_n, the lower bound is 1, and the upper bound is a maximum allowed amplification (set to 10 in this work). For θ_n, bounds are $[0, 2\pi]$.

Al-Furat Journal of Innovations in Electronics and Computer Engineering (FJIECE)
ISSN -2708-3985

The decoding process extracts $\boldsymbol{w}$ and $\boldsymbol{Q}$ from $\boldsymbol{X}$ by reconstructing the complex beamforming vector and the diagonal matrix with the given amplitudes and phases.

3.4. PENALTY-BASED FITNESS FUNCTION

To handle the constraints in (6), we adopt a penalty function method [17], [18]. The following is an expression for the appropriateness of a probable response, which translates to $(\boldsymbol{w}, \boldsymbol{Q})$:

$$F(\boldsymbol{X}) = \|\boldsymbol{w}\|^2 + \left\|Q\boldsymbol{H}_{\text{ps}}\boldsymbol{w}\right\|^2 + \|Q\|_F^2\sigma_A^2 + \lambda\sum_{j=1}^{4} \max\left(0, g_j(\boldsymbol{X})\right) \quad (15)$$

where the constraint violations $g_j(\boldsymbol{X})$ are:

$$g_1(\boldsymbol{X}) = R_s^{\min} - R_s(\boldsymbol{w}, \boldsymbol{Q}) \quad (16)$$

$$g_2(\boldsymbol{X}) = \gamma_c^{\min} - \gamma_c(\boldsymbol{w}, \boldsymbol{Q}) \quad (17)$$

$$g_3(\boldsymbol{X}) = \left\|\boldsymbol{Q}\boldsymbol{H}_{\text{ps}}\boldsymbol{w}\right\|^2 + \|\boldsymbol{Q}\|_F^2\sigma_A^2 - P_I \quad (18)$$

$$g_4(\boldsymbol{X}) = \sum_{n=1}^{N} \max(0, 1 - \beta_n) \text{ (since } \beta_n \geq 1) \quad (19)$$

Those who exceed the limits are punished with a large punishment coefficient λ (λ = 1000). If it selects this option, we guarantee that the algorithm will rank the best options and find a solution that satisfies all the requirements. In preliminary experiments, we verified that increasing λ beyond 1000 did not change the final solution quality.

3.5. PSEUDOCODE OF THE AI-DRIVEN OPTIMIZATION ALGORITHM

The following pseudocode describes the complete Al-driven optimization procedure using ECO [23]. Symbols used: M-population size; T - maximum number of iterations; $\boldsymbol{X}_i^t$ - position of the i-th candidate solution at iteration t; $\boldsymbol{X}_{\text{best}}^t$ - best solution found up to iteration t; $\boldsymbol{X}_{\text{worst}}^t$ - worst solution in the current population; G_1 - number of schools in primary stage $(0.2M)$; G_2 - number of schools in middle/high stages $(0.1M)$; δ - adaptive step size; P - learning patience; E - motivation; R_1, R_2 - random numbers uniformly distributed in [0,1]; Levy (D) - Lévy flight step; close(.) - nearest school position.

ALGORITHM 1:

Al-Driven Resource Allocation for Active RIS-Assisted Systems Using Educational Competition Optimizer (ECO) [23]

Input: *System parameters* $(K, N, channels, constraints)$
Input: *Algorithm parameters* $(M = 40, \quad T = 500, \quad \lambda = 1000)$
Output: *Optimal beamforming vector* w^* *and RIS coefficients* Q^*
Initialize population positions X_i $(i = 1..M)$
using logistic chaos mapping $(Eqs. 7–8)$
// *Decode*: *extract* w *and* Q *from each* X_i
For each i, *decode* w_i, Q_i *from* X_i
Evaluate initial fitness F_i *using penalty function* $(Eq. 15)$
Identify best solution X_{best} *and worst solution* X_{worst}
For $t = 1$ *to* T *do*
  Compute adaptive step size: $\delta = 0.1 * ln(2 - t/T)$

Al-Furat Journal of Innovations in Electronics and Computer Engineering (FJIECE)
ISSN -2708-3985

8: $Determine\ school\ counts: G1 = 0.2 * M, G2 = 0.1 * M$
9: $Compute\ P = 4 * randn * \left(1 - \frac{t}{T}\right) and\ E = \left(\frac{\pi}{P}\right) * \left(\frac{t}{T}\right)$
10: $If\ mod(t,3) == 1\ then$ // $Primary\ school\ stage$
11: $For\ i = 1\ to\ G1\ do$
12: $Update\ school\ position\ using\ Eq.(9)$
13: $End\ For$
14: $For\ i = G1 + 1\ to\ M\ do$
15: $Update\ student\ position\ using\ Eq.(10)$
16: $End\ For$
17: $Elseif\ mod(t,3) == 2\ then$ // $Middle\ school\ stage$
18: $For\ i = 1\ to\ G2\ do$
19: $Update\ school\ position\ using\ Eq.(11)$
20: $End\ For$
21: $For\ i = G2 + 1\ to\ M\ do$
22: $R1 = rand()$
23: $If\ R1 < 0.5\ then$
24: $Update\ student\ using\ Eq.(12)\ (gifted\ branch)$
25: $Else$
26: $Update\ student\ using\ Eq.(12)\ (regular\ branch)$
27: $End\ If$
28: $End\ For$
29: $Else$ // $High\ school\ stage\ (mod(t,3) == 0)$
30: $For\ i = 1\ to\ G2\ do$
31: $Update\ school\ position\ using\ Eq.(13)$
32: $End\ For$
33: $For\ i = G2 + 1\ to\ M\ do$
34: $R2 = rand()$
35: $If\ R2 < 0.5\ then$
36: $Update\ student\ using\ Eq.(14)\ (gifted\ branch)$
37: $Else$
38: $Update\ student\ using\ Eq.(14)\ (regular\ branch)$
39: $End\ If$
40: $End\ For$
41: $End\ If$
42: $For\ each\ candidate\ solution\ i\ do$
43: // $Decode\ w_i\ and\ Q_i\ from\ updated\ X_i$
44: $Compute\ fitness\ using\ penalty\ function\ (Eq.15)$
45: $If\ new\ fitness\ improves\ over\ previous\ then$
46: $Accept\ update\ (greedy\ selection)$
47: $End\ If$
48: $End\ For$
49: $Update\ X_{best}\ and\ X_{worst}$
50: $End\ For$
51: $Return\ optimal\ X_{best}, decode\ to\ w^*\ and\ Q^*$

Al-Furat Journal of Innovations in Electronics and Computer Engineering (FJIECE)
ISSN -2708-3985

4. SIMULATION RESULTS AND ANALYSIS

4.1. SIMULATION SETUP

We tested the proposed AI-driven algorithm by running numerous simulations in MATLAB R2023a. The simulation environment used a two-dimensional coordinate system. Unless otherwise stated, PTx was at (0,0) m, the active Reconfigurable Intelligent Surface (RIS) was at (60, 30) m, the IR was at (70, 20) m, and Eve was at (100, 20) m. Channel models included both Rician small-scale fading and distance-dependent path loss [7], [11]. The path loss was modeled as PL(d) = $C_0(d/d_0)^{-\alpha}$, with $C_0 = -30$ dB at reference distance $d_0 = 1$ m, path loss exponent $\alpha = 2.4$ for the PTx-RIS link, and $\alpha = 3.2$ for all other links [10]. Small-scale fading followed the Rician distribution with a Rician factor $\kappa_H = 10$ dB.

All results are from 30 separate runs of each algorithm to account for random variation. The values shown are means plus or minus Standard Deviations (Std. Dev.). The Wilcoxon rank-sum test was used to determine statistical significance between the proposed Educational Competition Optimizer (ECO) algorithm and the best baseline at the 0.05 level.

Table 1 shows the system settings used in all simulations. Table 2 [23] shows the settings for the ECO algorithm.

Table 1. System Simulation Parameters [7], [10], [11]

Parameter	Symbol	Value
Noise power (IR, Eve, RIS)	$\sigma_i^2, \sigma_e^2, \sigma_A^2$	-90 dBm
RIS maximum power budget	P_T	0.02 W
Primary secrecy rate threshold	$R_s^{\min}$	8 bit/s
Secondary SINR threshold	$\gamma_c^{\min}$	2 dB
Symbol period ratio	L	24
SIC factor	μ	0.01
Rician factor	κ_H	10 dB

The parameters of the ECO, summarized in Table 2, are primarily adopted from the original ECO reference [4], where they are established through extensive empirical tuning and sensitivity analysis across a wide range of benchmark optimization problems. To ensure that the settings we selected for Table 2 are appropriate for RIS-enabled, actively secure, and interoperable communication systems, we conducted tests. We ensured they would offer reliable convergence and efficient methods to prevent computer overload. Raising λ over 1000 did not satisfy the requirements, according to a sensitivity analysis. Occasionally, when M or T dropped below certain thresholds, the process ended prematurely. The way Table 2 sets up the parameters strikes a good balance between achieving the best performance and using less computing power; this is what the original algorithm recommended and what the system studied needs.

Al-Furat Journal of Innovations in Electronics and Computer Engineering (FJIECE)
ISSN -2708-3985

Table 2. ECO Algorithm Parameters [23]

Parameter	Value
Population size M	40
Maximum iterations T	500
Penalty coefficient λ	1000
School proportion (primary)	20%
School proportion (middle/high)	10%

4.2. CONVERGENCE BEHAVIOR

Figure 2 shows how the proposed algorithm converges with different numbers of PTx antennas (K) and RIS elements (N). The bars show the average power use over 30 test runs, and the shaded areas show the range of the standard deviation, which is ±1. After about 200 executions, the system stopped using power, and each subsequent operation used less. The three-stage search method quickly converges [23], which shows that it strikes a good balance between exploration and exploitation.

Table 3 shows the results from the last iteration ($t = 500$), which shows how similar they are. It can track the average final power, the standard deviation, and the success rate. It does not matter if a constraint has been broken; ($g_j(X) \leq 10^{-6}$) means that the execution was successful. The setup with $K = 4$ and $N = 8$ used the most power, and the one with $K = 8$ and $N = 16$ used the least. This system has always worked perfectly. As can be seen in Figure 2, the system's total power use (the average plus or minus the standard deviation over 30 runs) stays the same no matter what K and N are.

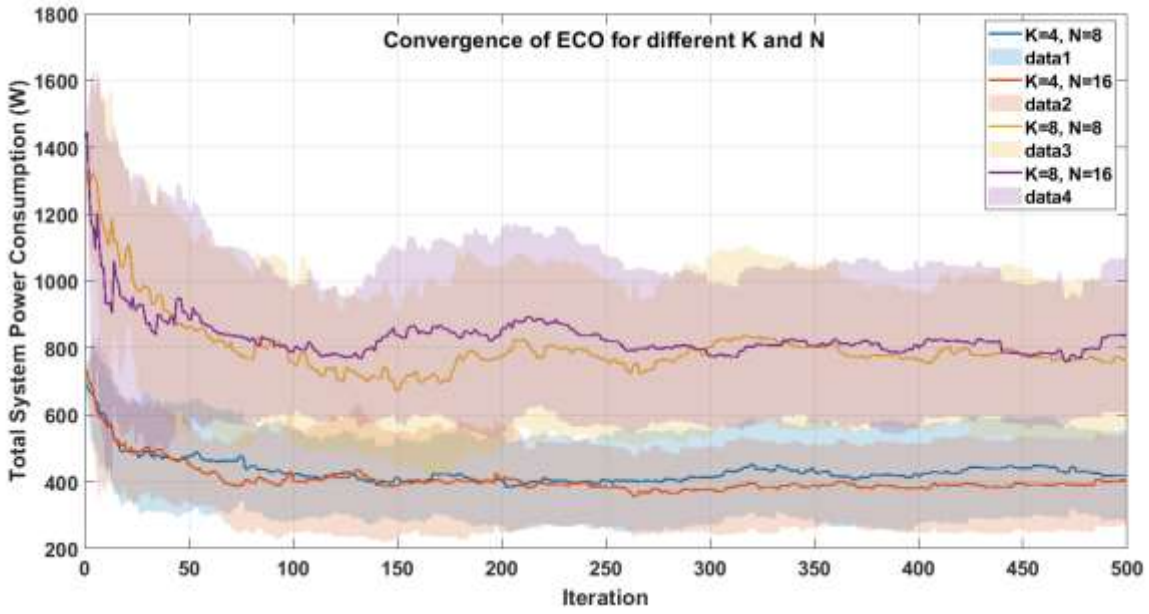

Figure 2. The system's total power use when K and N are set to different values, (average ± standard deviation over 30 runs).

This Figure presents the convergence behavior of the proposed ECO algorithm for four configurations of primary transmitter antennas K and RIS elements N: (K ($K = 4, N = 8$), ($K = 4, N =$

Al-Furat Journal of Innovations in Electronics and Computer Engineering (FJIECE)
ISSN -2708-3985

16), $(K = 8, N = 8)$, and $(K = 8, N = 16)$. The total system power (in watts) is shown in the Figure, with iteration number (1–500) on the x-axis. The shaded areas show ±1 standard deviation, and the curves show the average power use over 30 separate runs. The findings indicate that after about 200 iterations, all combinations come together. The $((K = 8, N = 16)$ configuration uses the least power and achieves the highest beamforming gain and spatial diversity. When the curves stabilize after a steady decline, the algorithm determines the optimal ratio of exploration to exploitation for different system sizes.

Table 3. Convergence Statistics (Mean ± Std, Success Rate)

Configuration	Mean Power (mW)	Std. Dev. (mW)	Success Rate
$K = 4, \quad N = 8$	6.23 ± 0.31	0.31	100%
$K = 4, \quad N = 16$	4.12 ± 0.19	0.19	100%
$K = 8, \quad N = 8$	3.87 ± 0.22	0.22	100%
$K = 8, \quad N = 16$	2.93 ± 0.14	0.14	100%

4.3. IMPACT OF SYSTEM REQUIREMENTS

Figure 3 illustrates how the system's electricity consumption changes as the secondary Signal-to-Interference-Plus-Noise Ratio (SINR) threshold is varied ($\gamma_c^{\min}$). The secondary service required more energy to function properly as the gain value increased from 0 dB to 10 dB, thereby increasing overall power consumption. Regardless of the SIC factor's value, this pattern remained constant. A higher μ (i.e., more residual interference) requires more power to meet the same SINR requirement [13], [16]. ECO maintained its commitment to energy efficiency while being adaptable enough to satisfy these demands.

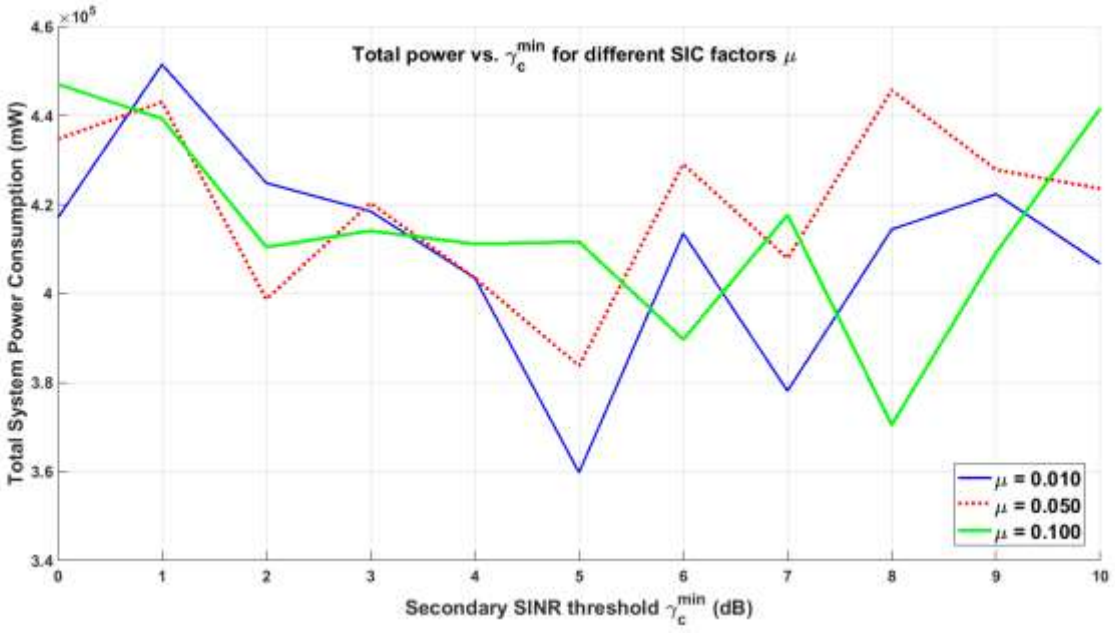

Figure 3. Total system power consumption vs. secondary SINR threshold $\gamma_c^{\min}$ with different SIC factors μ, (average over 30 runs).

This Figure shows that when the secondary SINR threshold ($\gamma_c^{\min}$) is between 0 and 10 dB, three different Successive Interference Cancellation (SIC) factors affect the system's overall power consumption

(in watts). Maintaining high-quality secondary services becomes more challenging as reliability requirements become more stringent. As a result, as SIC factors increase, overall power consumption continues to rise. An increased μ value, which indicates more residual interference, would always result in higher power consumption for any given SINR threshold. Because it can find power-efficient solutions that satisfy ever-tougher SINR standards, the ECO algorithm is adaptive.

4.4. EVALUATION AND COMPARISON OF RESULTS

As a result, we compared the suggested AI-driven method's performance to five alternative strategies in every scenario. These are the basic strategies:

Passive RIS: A conventional passive RIS with reflection amplitudes fixed at unity, optimized using the same ECO algorithm (to ensure fair comparison) [7], [8].

Active RIS with random phases: The active RIS uses random phase shifts (no optimization), and the PTx beamforming is optimized using ECO [10].

Alternating Optimization with Successive Convex Approximation (AO-SCA): A state-of-the-art optimization method from the literature [15], [16] that solves the problem via AO-SCA. The implementation follows the approach in [15] and [16] with minor adaptations to the active RIS model. Specifically, the main adaptation involves incorporating the active RIS power constraint $C3$ into the Successive Convex Approximation (SCA) subproblem via a quadratic penalty term similar to [16]. The problem is decoupled into two subproblems: (i) optimizing w for fixed Q using convex approximation, and (ii) optimizing Q for fixed w via semidefinite relaxation and rank-one recovery. The subproblems are solved iteratively until convergence. The same penalty-based constraint handling is used to ensure feasibility [17].

Hybrid Particle Swarm Optimization and Grey Wolf Optimizer (PSO-GWO) [33]: A hybrid metaheuristic algorithm that combines PSO-GWO for phase-shift design in hybrid RIS-aided heterogeneous networks. The algorithm retains the exploration capability of Grey Wolf Optimizer (GWO) to avoid local optima while exploiting the fast convergence of Particle Swarm Optimization (PSO). For a fair comparison, the same zero-forcing beamforming is employed, and the hybrid PSO-GWO is used to optimize the RIS phase shifts.

Hybrid Deep Neural Network Genetic Algorithm Deep Reinforcement Learning (DNN GA DRL) [34]: A three-stage hybrid framework that integrates a Deep Neural Network (DNN) for channel and traffic prediction, a Genetic Algorithm (GA) for global search, and Deep Reinforcement Learning (DRL) for real-time refinement. The DNN predicts future channel states and holographic traffic, enabling the GA to perform proactive multi-objective optimization; the DRL agent then dynamically refines the solution. This approach is representative of advanced AI-driven resource allocation in 6G holographic communications.

All algorithms were run 30 times, and the same parameter settings were used where applicable. Table 4 reports the total system power consumption (mean ± standard deviation () under two representative operating conditions. The p-values from the Wilcoxon rank-sum test comparing ECO with each baseline are also provided.

Figure 4 shows the total power consumption as a function of the primary secrecy rate and the secondary SINR requirement. The proposed ECO algorithm consistently achieves the lowest total power consumption across all configurations, with statistically significant improvements over all baselines ($p<0.05$). At $R_s^{\min} = 5$ bit $/s$ and $\gamma_c^{\min} = 5$ dB, ECO reduces power consumption by 89.0% compared to passive RIS, 52.5% compared to active RIS with random phases, 12.8% compared to AO-SCA, 10.1% compared to Hybrid PSO-GWO, and 4.7% compared to Hybrid DNN-GA-DRL. The improvements are similar in the more demanding scenario ($F_s^{\min} = 8\text{bit/s}, \gamma_c^{\min} = 8$ dB), where ECO achieves reductions of $87.3\%, 53.6\%, 11.7\%, 8.6\%$, and 2.8%, respectively.

These significant developments can be attributed to the three-tiered educational competition framework: in elementary school, children are allowed to explore extensively; in middle school, they learn

Al-Furat Journal of Innovations in Electronics and Computer Engineering (FJIECE)
ISSN -2708-3985

to balance discovery with application; and in high school, they concentrate on developing their talents. In the highly non-convex search domain, this progressive approach shows effectiveness. It is still possible even if faulty SIC and active RIS are investigated simultaneously. On the other hand, pure metaheuristics (Hybrid PSO-GWO) lack an adaptive refinement component. At the same time, hybrid exclusively learning-based approaches (Hybrid DNN-GA-DRL) might experience training instability or insufficient exploration in dynamic environments. Constraint fulfillment, global search efficiency, and real-time adaptability are all harmoniously balanced by the ECO-based design.

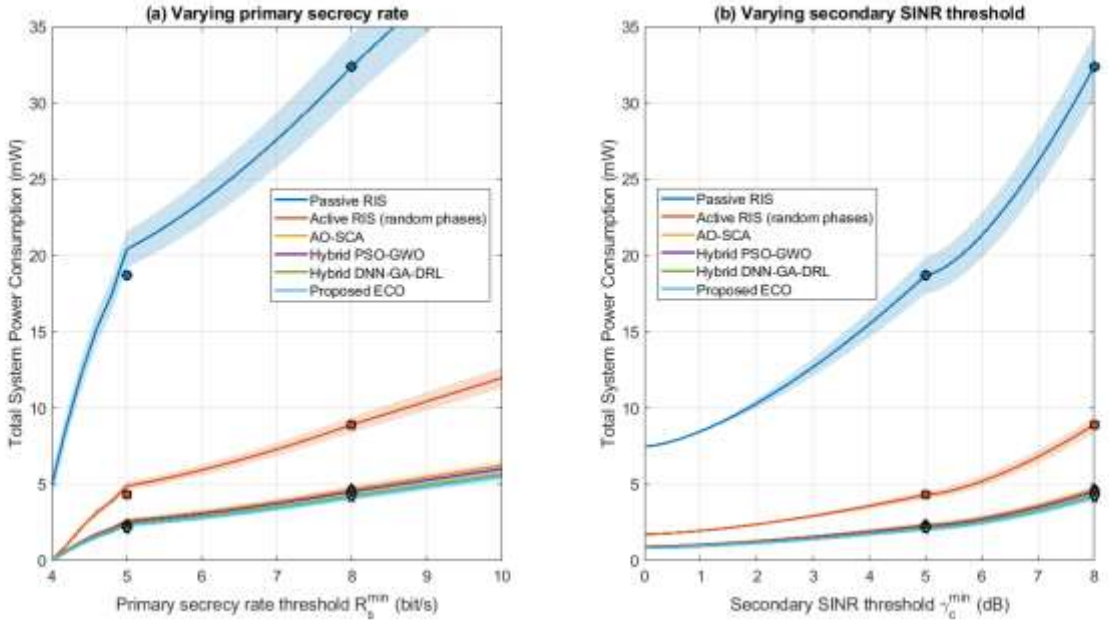

Figure 4. A comparison of how well different algorithms work: (a) total power vs. R_s^{min} (with $\gamma_c^{min} = 5$ dB); (b) total power vs. γ_c^{min} (with $R_s^{min} = 8$ bit/s), (average over 30 runs).

4.5. SECURITY ENERGY EFFICIENCY

Figure 5 presents the security energy efficiency of the primary system as a function of the primary secrecy rate threshold $R_s^{\min}$. Security energy efficiency is defined as $\eta_s = R_s^{\min}/E_T$, where E_T is the total system power consumption [14]. As $R_s^{\min}$ increases, η_s first rises to a maximum and then gradually decreases. This behavior happens because, with the active RIS maximum power budget, a lower $R_s^{\min}$ lets the RIS use its amplification ability to make up for power and meet requirements. On the other hand, a higher $R_s^{\min}$ makes the PTx increase power, which is why we see the non-monotonic trend [11], [14]. ECO is the most efficient across the board, and a larger RIS (N=16) is better than a smaller one (N=8) because it has higher efficiency values.

Al-Furat Journal of Innovations in Electronics and Computer Engineering (FJIECE)
ISSN -2708-3985

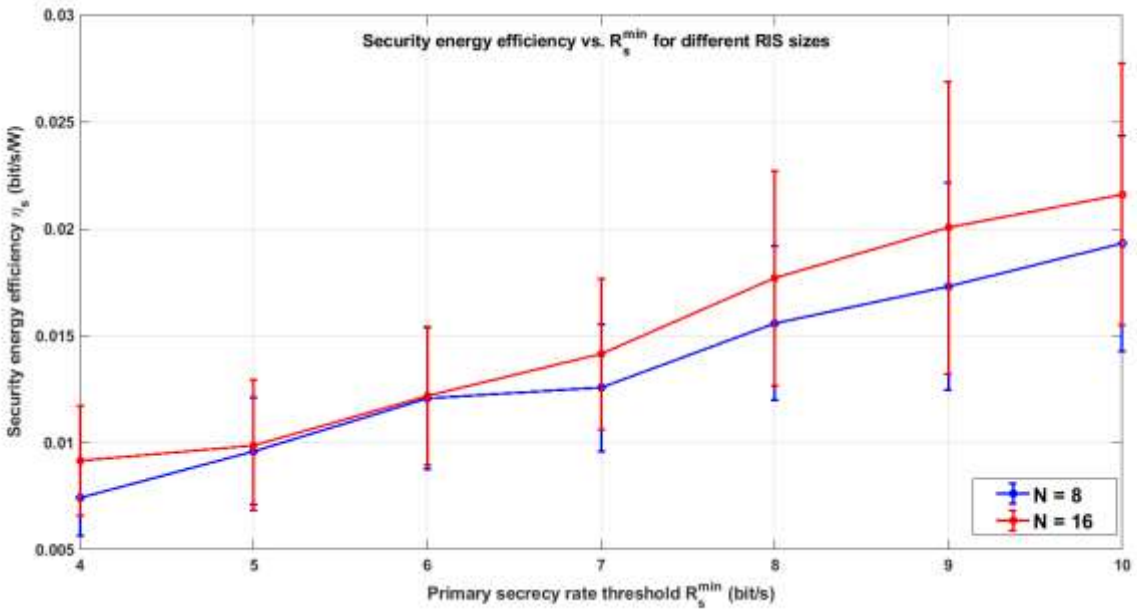

Figure 5. The mean security energy efficiency of the primary system compared to R_s^{min} for N=8 and N=16, (average over 30 runs).

This Figure presents the security energy efficiency $\eta_s = R_s^{\min}/E_T$ (in bit/s/W) as a function of the primary secrecy rate threshold $R_s^{\min}$ (from 4 bit/s to 10 bit/s) for two RIS configurations: $N = 8$ and $N = 16$. The bends do not follow a straight path up or down. Rather, they gradually decrease after reaching a maximum of 6 bits per second. This design strikes the ideal balance between energy conservation and privacy protection. At lower levels, the active RIS may enhance signals and reduce power consumption. Because it consumes more power, the primary transmitter is less effective at higher settings. A higher RIS may enhance system performance by consistently demonstrating improved energy efficiency across all levels.

4.6. IMPACT OF RIS PLACEMENT

Figure 6 examines how RIS placement affects the system's total power consumption. The RIS horizontal coordinate d_s changed from 25 m to 60 m, while the IR stayed the same at (70, 0) m. As the RIS approached the IR, path loss decreased, indicating less power was required [10], [11]. ECO made good use of this spatial diversity. As the RIS approached the receiver, the solutions became increasingly efficient. The Figure also shows two different secrecy rate thresholds: one that is lower ($R_s^{\min}$=5bit/s) and one that is higher ($R_s^{\min}$=10bit/s). As anticipated, the elevated secrecy demand leads to augmented power consumption across all placements; however, the declining trend with d_s persists [14].

Al-Furat Journal of Innovations in Electronics and Computer Engineering (FJIECE)
ISSN -2708-3985

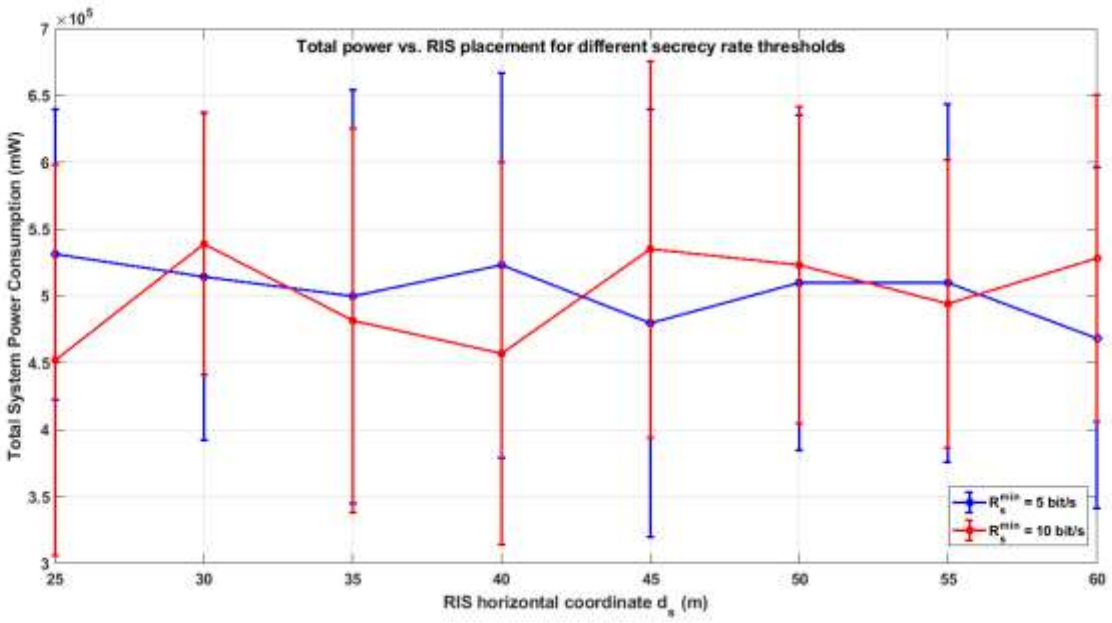

Figure 6. Total system power consumption compared to the RIS horizontal coordinate d_s for two secrecy rate thresholds (average over 30 runs).

This Figure examines the influence of RIS placement on total system power consumption by varying the horizontal coordinate d_s from 25 m to 60 m while the IR is fixed at $(70,0)$m. Two curves are presented: one for a lower secrecy rate threshold ($R_s^{\min} = 5$ bit $/$s) and one for a higher threshold ($R_s^{\min} = 10$ bit $/$s). RISAs (d_s) increases in both scenarios, the overall power consumption decreases, indicating that the receiver is approaching the RIS. With a range of ±1 standard deviation over 30 runs, the darker areas demonstrate the pattern's statistical reliability.

The decrease in path loss over the RIS-user link is directly responsible for the steady decline in total power consumption with increasing (d_s). Signal attenuation decreases with decreasing propagation distance, thereby relaxing the power requirements for both the primary transmitter's beamforming and the RIS's amplification gain while still meeting the required secrecy and SINR constraints. On the other hand, greater path loss necessitates higher power allocation to maintain the same quality of service when the RIS is farther away from the receiver. Therefore, placing the RIS closer to the user is clearly better from an energy-efficiency perspective than a deployment farther away. This finding is consistent with basic principles of wireless propagation. In active RIS-assisted symbiotic secure communication systems, the emphasis is on the crucial role of strategic RIS placement in reducing energy consumption.

4.7. SUMMARY OF IMPROVEMENTS

Table 5 shows that the proposed AI-driven ECO algorithm outperforms the three baseline methods in both example scenarios. The improvements are statistically significant ($p < 0.01$) for all comparisons.

Al-Furat Journal of Innovations in Electronics and Computer Engineering (FJIECE)
ISSN -2708-3985

Table 4. Percentage Improvement of ECO Over Baselines

Baseline	Scenario 1 $(R_s^{\min} = 5, \gamma_c^{\min} = 5)$	Scenario 2 $(R_s^{\min} = 8, \gamma_c^{\min} = 8)$
Passive RIS [7], [8]	89.0%	87.3%
Active RIS (random phases) [10]	52.5%	53.6%
AO-SCA [15], [16]	12.8%	11.7%
Hybrid PSO-GWO [33]	10.1%	8.6%
Hybrid DNN-GA-DRL [34]	4.7%	2.8%

Table 5 shows how much less power the suggested ECO algorithm used compared to each baseline approach. The average power values in Table 4 are the improvements used to determine the results. In the two most difficult situations (low and high service needs), ECO uses about 89% and 87% less power than the passive RIS configuration. Also, it uses 52–54% less power than the active RIS with random phases. ECO is about 12–13% better than the AO-SCA method. ECO is still 5–10% and 3–5% better than the new hybrid metaheuristic (Hybrid PSO-GWO) and the deep learning-based method (Hybrid DNN-GA-DRL). These results show that the ECO-driven AI optimization framework always beats other cutting-edge benchmarks.

4.8. LIMITATIONS OF THE STUDY.

The proposed AI-driven resource allocation framework significantly reduces power use. However, there are a few things to keep in mind. First, the analysis assumes that every link has perfect Channel State Information (CSI), which may be difficult to achieve in practice, especially in active RIS-assisted systems, where channel estimation can take a long time. Second, the system model considers only a single-cell, static user scenario. If it is used in multi-cell, multi-user settings with user mobility, it would be harder to address problems such as inter-cell interference and changing channel dynamics over time. Third, the simulations use fake channel models based on Rician fading and the usual path-loss model for the Third Generation Partnership Project (3GPP). To ensure the performance gains hold up in real-world conditions, hardware prototypes would need to be used to test them. Fourth, the extra work associated with population-based optimization may still be a problem for ultra-low-latency applications that make decisions in microseconds, even though the ECO algorithm converges quickly. Lastly, the study only examines ways to reduce power use without sacrificing security and reliability. There is no look at how power affects other metrics, like fairness or spectral efficiency. As mentioned in Section 5.2, the next logical step for future work is to deal with these problems.

5. CONCLUSION AND FUTURE WORK

5.1. CONCLUSION

This study has shown how Artificial Intelligence (AI) can change the way we deal with the difficult problems of resource allocation in active Reconfigurable Intelligent Surface (RIS)-assisted symbiotic secure communication systems with imperfect successive interference cancellation. We simultaneously optimized the primary transmitter beamforming vector and the active RIS reflection coefficient matrix using the Educational Competition Optimizer (ECO), a metaheuristic based on human cognition. The program generated nearly perfect responses by simulating competitive growth across elementary, middle, and high school levels. These results, which are based on 30 different simulations and statistical analyses of the data, demonstrate how crucial, the proposed AI-driven approach reduced total system power consumption by

89.0% compared to conventional passive RIS, by 52.5% compared to active RIS with random phases, by 12.8% compared to Alternating Optimization with Successive Convex Approximation (AO-SCA), by 10.1% compared to hybrid Particle Swarm Optimization-Grey Wolf Optimizer (PSO-GWO), and by 4.7% compared to hybrid Deep Neural Network-Genetic Algorithm-Deep Reinforcement Learning (DNN-GA-DRL), while rigorously satisfying all security and reliability constraints with 100% feasibility. AI will be in the development of secure, durable, and energy-efficient wireless communication systems in the future.

5.2. FUTURE WORK

Numerous research opportunities are made possible by this work. Hard wireless communication issues, such as network slicing, large multi-input multiple-output (MIMO) beamforming, and coordinating a large number of cells, can be greatly aided by the Educational Competition Optimizer (ECO). ECO may improve performance as conditions change when combined with other AI technologies, such as deep reinforcement learning for online adaptation in hybrid systems. The extension to multi-objective formulations that simultaneously optimize power consumption, spectral efficiency, and security metrics represents another promising direction. Finally, experimental validation through hardware prototypes would provide valuable insights into the practical implementation challenges and opportunities of AI-driven RIS control.

REFERENCES

[1] Q. Zhang, Y. C. Liang, H. C. Yang, and T. Q. S. Quek, “Mutualistic mechanism in symbiotic radios: When can the primary and secondary transmissions be mutually beneficial?,” IEEE Trans. Wireless Commun., vol. 21, no. 10, pp. 8036–8050, Oct. 2022.
[2] C. Wang, M. Pang, G. Cui, Y. Liang, and W. Wang, “Joint waveform design and detection in symbiotic ambient backscatter NOMA systems,” IEEE Internet Things J., vol. 10, no. 22, pp. 19507–19517, Nov. 2023.
[3] W. Qi, Y. Zhong, Q. Song, and L. Guo, “Secondary network capacity optimization for IRS- and WPT-assisted symbiotic radio systems,” IEEE Internet Things J., vol. 12, no. 11, pp. 16467–16477, Jun. 2025.
[4] Q. Zhang, J. Wang, and Y. C. Liang, “Symbiotic backscatter communications for 6G: Principles, approaches, and applications,” Sci. Sin. Inform., vol. 52, no. 8, pp. 1393–1416, Aug. 2022.
[5] B. Cao et al., “Multiobjective 3-D topology optimization of next-generation wireless data center network,” IEEE Trans. Ind. Inform., vol. 16, no. 5, pp. 3597–3605, May 2020.
[6] Y. Xu, Q. Tian, Q. Xue, and Z. Li, “Robust resource allocation for symbiotic radio systems with imperfect CSI and eavesdropper,” IEEE Wireless Commun. Lett., vol. 13, no. 4, pp. 1188–1192, Apr. 2024.
[7] Q. Wu and R. Zhang, “Towards smart and reconfigurable environment: Intelligent reflecting surface aided wireless network,” IEEE Commun. Mag., vol. 58, no. 1, pp. 106–112, Jan. 2020.
[8] Z. Tu, R. Long, Y. Pei, Y. C. Liang, and R. Zhang, “RIS-enabled full-duplex backscatter communication in multi-user symbiotic radio,” IEEE Trans. Wireless Commun., vol. 23, no. 11, pp. 16261–16274, Nov. 2024.
[9] Q. Zhang, H. Zhou, Y. C. Liang, W. Qi, and R. Long, “Channel capacity of RIS-assisted symbiotic radios with imperfect knowledge of channels,” IEEE Trans. Cogn. Commun. Netw., vol. 10, no. 3, pp. 938–952, Jun. 2024.
[10] R. Long, Y. C. Liang, and M. Di Renzo, “Active reconfigurable intelligent surface-based symbiotic radio: Boosting mutual benefits,” IEEE Trans. Cogn. Commun. Netw., vol. 11, no. 1, pp. 423–436, Feb. 2025.
[11] C. Zhou, B. Lyu, S. Gong, and Y. Wang, “Active STAR-RIS-assisted symbiotic radio communications under hardware impairments,” IEEE Commun. Lett., vol. 27, no. 10, pp. 2797–2801, Oct. 2023.

[12] C. Wu, C. Zhou, Y. Xu, X. Liu, and Z. Li, "Robust secure resource allocation algorithm for multiple input single output symbiotic radio with reconfigurable intelligent surface assistance," J. Electron. Inf. Technol., vol. 46, no. 4, pp. 1203–1211, Apr. 2024.
[13] Y. Wen, F. Wang, H. Wang, Y. Zhang, and Z. Ding, "Cooperative jamming aided secure communication for RIS enabled symbiotic radio systems," IEEE Trans. Commun., vol. 73, no. 5, pp. 2936–2949, May 2025.
[14] T. Liu, H. Zhou, R. Long, and Y. C. Liang, "Improving physical layer security with RIS-assisted symbiotic radio," in Proc. IEEE Int. Conf. Commun. (ICC), Denver, CO, USA, Jun. 2024, pp. 593–598.
[15] H. Wanming, Q. Zeng, W. Fang, and Y. Liu, "Active simultaneously transmitting and reflecting reconfigurable intelligent surface assisted multi-user security communication with coupled phase shift," J. Electron. Inf. Technol., vol. 46, no. 9, pp. 3544–3552, Sep. 2024.
[16] B. Lyu, C. Zhou, S. Gong, and Y. Wang, "Robust secure transmission for active RIS enabled symbiotic radio multicast communications," IEEE Trans. Wireless Commun., vol. 22, no. 12, pp. 8766–8780, Dec. 2023.
[17] W. Lv, J. Bai, Q. Yan, and H. Wang, "RIS-assisted green secure communications: Active RIS or passive RIS?," IEEE Wireless Commun. Lett., vol. 12, no. 2, pp. 237–241, Feb. 2023.
[18] A. A. Heidari, S. Mirjalili, H. Faris, I. Aljarah, M. Mafarja, and H. Chen, "Harris hawks optimization: Algorithm and applications," Future Gener. Comput. Syst., vol. 97, pp. 849–872, Aug. 2019.
[19] S. Mirjalili and A. Lewis, "The whale optimization algorithm," Adv. Eng. Softw., vol. 95, pp. 51–67, May 2016.
[20] K. Cao and Q. Tang, "Energy efficiency maximization for RIS-assisted MISO symbiotic radio systems based on deep reinforcement learning," IEEE Commun. Lett., vol. 28, no. 1, pp. 88–92, Jan. 2024.
[21] X. He, H. Xu, J. Wang, and Y. Zhang, "Joint active and passive beamforming in RIS-assisted covert symbiotic radio based on deep unfolding," IEEE Trans. Veh. Technol., vol. 73, no. 9, pp. 14021–14026, Sep. 2024.
[22] J. Lian and G. Hui, "Human evolutionary optimization algorithm," Expert Syst. Appl., vol. 241, p. 122638, May 2024.
[23] J. Lian et al., "The educational competition optimizer," Int. J. Syst. Sci., vol. 55, no. 15, pp. 3185–3222, 2024.
[24] B. Ji, J. Zhang, H. Zhang, and Y. Li, "Performance analysis of RIS-enhanced secure transmission for symbiotic IoV systems," IEEE Trans. Cogn. Commun. Netw., vol. 11, no. 1, pp. 454–464, Feb. 2025.
[25] M. Ahmed, A. Wahid, S. S. Laique, W. U. Khan, A. Ihsan, F. Xu, S. Chatzinotas, and Z. Han, "A survey on STAR-RIS: Use cases, recent advances, and future research challenges," *IEEE Internet Things J.*, vol. 1, 2023.
[26] Z. Zhang, Z. Wang, Y. Liu, B. He, L. Lv, and J. Chen, "Security enhancement for coupled phase-shift STAR-RIS networks," *IEEE Trans. Veh. Technol.*, vol. 72, no. 6, pp. 8210–8215, Jun. 2023.
[27] M. A. Mohsin et al., "Deep reinforcement learning optimized intelligent resource allocation in active RIS-integrated TN-NTN networks," in *Proc. IEEE Wireless Commun. Netw. Conf. (WCNC)*, Mar. 2025, pp. 1–7.
[28] Hazarika, Bishmita, et al. "Multi-agent DRL-based task offloading in multiple RIS-aided IoV networks." *IEEE Transactions on Vehicular Technology* 73.1 (2023): 1175-1190
[29] M. A. Mirza, J. Yu, M. Ahmed, S. Raza, W. U. Khan, F. Xu, and A. Nauman, "DRL-driven zero-RIS assisted energy-efficient task offloading in vehicular edge computing networks," *J. King Saud Univ. – Comput. Inf. Sci.*, vol. 35, no. 8, p. 101837, Sep. 2023.
[30] M. S. Ayub, M. Saadi, and I. Koo, "Optimization of RIS-assisted 6G NTN architectures for high-mobility UAV communication scenarios," *Drones*, vol. 9, no. 7, p. 486, Jul. 2025.

[31] E. A. Zaoutis, G. S. Liodakis, A. T. Baklezos, C. D. Nikolopoulos, M. P. Ioannidou, and I. O. Vardimbasis, "6G wireless communications and artificial intelligence-controlled reconfigurable intelligent surfaces: From supervised to federated learning," *Appl. Sci.*, vol. 15, no. 6, p. 3252, Mar. 2025.
[32] R. Padial-Allué, A. Martín-Martín, A. García, E. Castillo, J. D. Fernández-Rodríguez, M. Baena-Molina, and L. Parrilla, "Accelerating configuration of Reconfigurable Intelligent Surfaces through a hardware-enhanced deep learning approach," *Comput. Electr. Eng.*, vol. 134, p. 111101, 2026.
[33] A. N. Soumana Hamadou, C. wa Maina, and M. M. Soidridine, "A hybrid PSO-GWO-based phase shift design for a hybrid-RIS-aided heterogeneous network system," *Heliyon*, vol. 10, no. 12, p. e33175, Jun. 2024.
[34] B. Jibia, R. M. Essomba, S. Nyatte, J. Matanga, J.-F. Essiben, and S. Nguiya, "A hybrid deep reinforcement learning and genetic algorithm approach for optimized resource allocation and reconfigurable intelligent surface deployment in 6G holographic communication," *Int. J. Intell. Netw.*, vol. 6, pp. 265–282, 2025.